Congshan Li[1]
Yan Fang[2,*],
Shaoyu Shi[3],
Ping He[4]
Tingyu Sheng[5]
Yikai Li[6]

J. Electrical Systems 16-3 (2020): 295-307

Regular paper

Analysis on damping characteristics of hybrid multi-infeed DC system with wind farm

The interaction between AC and DC systems in hybrid multi-infeed direct current (HMIDC) system has a significant effect on the damping characteristics of the system, meanwhile, the doubly-fed induction generator (DFIG)-based wind turbine (WT) makes the system's structure more complicated. It is challenging to analyze the system's stability quantitatively. In this article, wind power joined the HMIDC system. Then, based on the basic principle of wind generation and low frequency oscillation (LFO) the influence of the WT's access points and the capacity of the WT on the damping characteristics and stability of the system is studied. Based on the total least squares-estimation of signal parameters via rotational invariance techniques (TLS-ESPRIT) algorithm, and the system eigenvalue, frequency, damping ratio, and other information are obtained. The analysis shows that when the WT is incorporated into different HMIDC system positions, the system has different oscillation modes and damping ratios. And in these oscillation modes, the damping ratio gradually decreases with increasing oscillation frequency. When the capacity of the WT is increased, the change of damping ratio is not apparent than before. The eigenvalue analysis is well verified by simulation analysis on the PSCAD/EMTDC platform.

Keywords: Damping characteristics; hybrid multi-infeed DC power transmission system; low frequency oscillation; doubly-fed induction generator-based wind turbine.

Article history: Received 27 November 2019, Accepted 4 June 2020

1. Introduction

The 19th National Congress of the Communist Party of China came up with the task of "implementing the new development concept, building a modern economic system", and "building and improving the economic system of green and low-carbon recycling development". It can be seen that China attaches great importance to the development of new energy source. Wind power and conventional energy have different grid-connected mode because of the random nature of wind energy. Wind power has a higher standard on the operation mode of the electric system. With the growing of the wind turbine (WT) capacity and the boost in grid voltage level, changes in the operation have brought severe challenges to the electric network. In addition, the interactions between wind power and grid not only led to kinds of oscillation modes but also have an effect on the damping characteristics of the grid.

For wind power grid-connected, high-voltage direct current (HVDC) system is the best choice as an ideal power grid structure. Therefore, wind power is generally transported by DC. Recently, with the increasing application of DC transmission, a hybrid multi-infeed direct current system (HMIDC) has been formed, which is consist of voltage source converter based high voltage direct current (VSC-HVDC) and line commutated converter based high voltage direct current (LCC-HVDC). The two are fed into the same power system with close electrical distance. Thus, the HMIDC system containing wind power will

[*] Corresponding author: Department of Electrical and Information Engineering, Zhengzhou University of Light Industry, Zhengzhou, Henan, 450002, PRC, E-mail: 498947468@qq.com
[1.2.4.5.6]Department of Electrical and Information Engineering, Zhengzhou University of Light Industry, Zhengzhou, 450002 P.R. China
[3] Sanmenxia power supply company of State Grid Henan Electric Power Company, Sanmenxia, P.R. China

be formed. The extensive integration of WT in the HMIDC system has respectively led to the interactions between the wind farm and the VSC-HVDC, LCC-HVDC and the grid more complicated, which will cause the power system to produce various oscillation modes.

As an extensively used WT, doubly-fed induction generator (DFIG)-based WT, its stator and rotor winding joined the power system. And the rotor winding joined the system via AC/DC converter to provide AC excitation, which can realize constant frequency power generation at different speeds. However, the connection mode of DFIG-based WT will have an impact on the system oscillation mode [1]. In [2], the influence of DC system integration into the grid on the small signal stability of AC network is studied in the HMIDC system with DFIG-based WT, but the impact on the grid's oscillation mode and damping characteristics which is related to the selection of the WT's location is not considered. In [3], using the eigenvalue method to analyze the small signal stability and damping characteristics of the DFIG-based WT joined the infinite-bus network, and the cause of the system oscillation is obtained by eigenvalue calculation. This agrees with the finding with [4], which analyzed the influence of WT on sub-synchronous oscillation mode using eigenvalues, and explored the influence of different participation factors on sub-synchronous oscillation. In [5], the selection of wind turbine's access point is considered. Through eigenvalue analysis and time-domain simulation for different operating conditions with fault, this article studied the change of system's damping characteristics with the increase of WT output and the influence of DFIG-based WT output on small signal stability and transient stability of the network. The placement of DFIG has a great effect on the system's LFO damping by using eigenvalue analysis [6]. In [7], the interactions between the DFIG-based WT and the synchronous generator are revealed in terms of the output dynamics of the PLL, and its damping characteristics is related to the oscillation frequency. [8] proposed that the mutual effect between DFIG-based WT and the HVDC is unapparent while the damping becomes weak with the increase of wind farm capacity.

In addition, lots of study has been carried out to evaluate the suppression methods of various oscillation modes in the power grid, and the corresponding controllers are designed.

The different operation mode, wind farm's capacity size and the change of power flow when the wind farm joined the system will have an effect on the LFO characteristics in the system [9]. In [10], the model of VSC-HVDC system with DFIG-based WT is built, and analysis the influence of factor such as the number of DFIG-WTs, wind speed and other parameters on the SSO characteristics. But it only considered the VSC-HVDC system. Utilizing TLS-ESPRIT technology and improved projective theorem, a reduced-order DC additional damping controller is designed to suppress LFO. But other eigenvalues are introduced in the selection process, which causes the algorithm more complicated [11]. A coordinated control method of PSS and power oscillation dampers (PODs) of DFIG is proposed. An appropriate location of access point of wind farm is found by using eigenvalue analysis. It's for IEEE 68 bus test system [12].

Considering the system's coupling relationship between LFO and sub-synchronous oscillation, the damping controller designed by the mode separation method in [13] can transform the coupling problem into the parameter optimization problem of the controller and improve the damping characteristics of the system. According to cloud computing theory, a coordinated optimization strategy of multi-channel power system static (PSS)

controller and Thyristor controlled series capacitor (TCSC) is proposed in [14], which has a significant impact in suppressing LFO and sub-synchronous oscillation. In [15], H_∞ mixed-sensitivity robust controller is designed to suppress LFO damping. The result shows that the controller designed by this article has a good robust performance with the wind speed variation. In addition, the oscillation modes identified by TLS-ESPRIT are decomposed into multiple channels, and each channel is optimized by using the adaptive algorithm to suppress the system's LFO and sub-synchronous oscillation [16].

According to the current research reports, there are few works of literature to study the multi-band oscillation (MBO) of DFIG-based WT incorporated into the power grid through VSC-HVDC sending end, LCC-HVDC sending end and power grid receiving end [17]. As can be seen from the above background, this paper first establishes the HMIDC system with DFIG-based WT, and studies the influence of WT's access point on the damping characteristics and stability of the system after the parallel connection of the DFIG-based WT to the HMIDC system. The DFIG-based WT is connected to power grid from VSC-HVDC, LCC-HVDC and power system，respectively. Through building the system model on PSCAD / EMTDC simulation platform and simulating, the corresponding power angle curve is obtained. The eigenvalue is obtained by TLS-ESPRIT algorithm, and the influence of the access point and capacity of WT on the system oscillation characteristics is obtained by eigenvalue analysis. This research can provide corresponding technical support for wind power grid planning.

2. DFIG-based WT model

The main components of the DFIG-based WT are the WT part, the asynchronous motor part and the converter part. The WT is mainly composed of a wind wheel, a gearbox and a transmission shaft. The wind power drives the mechanical power generated by the rotation of the wind wheel and is transmitted to the rotor side of the generator to drive the rotation, thereby realizing the conversion of wind power to mechanical power, and realizes the mechanical power to the electric power through the mutual cooperation of the dual PWM converter and the control system. The WT stator and rotor are joined to the system, respectively, but the rotor joins the system via a PWM inverter. The magnitude, frequency and phase of the rotor excitation current amplitude are realized by adjusting the AC excitation so that the active and reactive power of unit output can be realized. Decoupling control and reducing the damping of the corresponding oscillation mode is not conducive to suppressing system oscillation. In Figure 1, the structure of the DFIG-based WT is as follows.

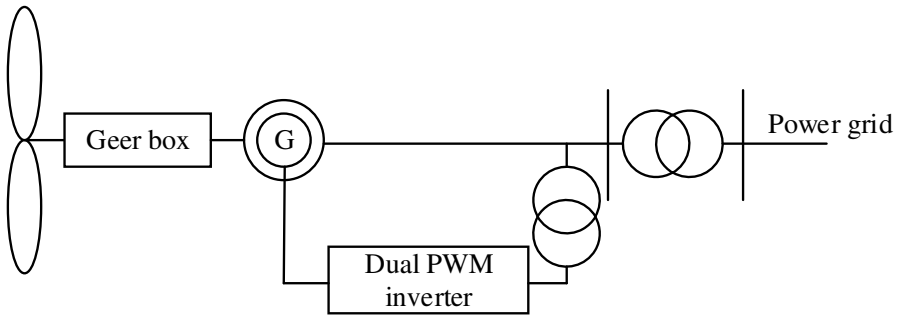

Figure 1. The DFIG-based WT model

The DFIG-based WT has noticeable advantages as follow:

1) The constant frequency power generation at different speeds is mainly achieved by setting the frequency of the excitation current. The economic operation of the unit is realized by the most efficient utilization of energy;

2) Decoupling control of active and reactive power is realized, and the reactive power demand of the power system is compensated by setting the power factor of the system;

3) Due to the excitation current adjusted by the grid voltage, current and generator speed, the DFIG-based WT can accurately adjust the generator output voltage;

4) Reduce the capacity and cost of the inverter.

The oscillation characteristics between large-scale power system regions and their internals are related to the structure and damping characteristics of the power grid. The type of WT, grid-connected mode, grid-connected capacity, and grid-connected access points will have different influences on damping characteristics of the grid.

2.1 Mathematical model of DFIG-based WT

The DFIG-based WT model is made up of voltage equation, flux linkage equation and torque equation. For analysis, the model analysis needs to be based on certain assumptions. The details are illustrated in [18]. Using the DFIG-based WT in abc static coordinate system to deal with the problem, the calculation will be particularly difficult to solve, so coordinate transformation is chosen to simplify the model. That is, the mathematical model is converted by using the Park transformation.

The DFIG-based wind turbines' voltage equation is

$$u_{sd} = R_s i_{sd} + \rho\psi_{sd} - \omega_1\psi_{sq} \tag{1}$$

$$u_{sq} = R_s i_{sq} + \rho\psi_{sq} + \omega_1\psi_{sd} \tag{2}$$

$$u_{rd} = R_r i_{rd} + \rho\psi_{rd} - \omega_s\psi_{rq} \tag{3}$$

$$u_{rq} = R_r i_{rq} + \rho\psi_{rq} + \omega_s\psi_{rd} \tag{4}$$

where u_{sd}, u_{sq} are the stator voltage of $d-$ and $q-$axis, u_{rd}, u_{rq} are the rotor voltage of $d-$and $q-$axis, i_{sd}, i_{sq} are respectively the stator current of $d-$and $q-$axis, i_{rd}, i_{rq} are the rotor current $d-$ and $q-$axis, ρ is the differential operator, R_s, R_r are the resistance of stator and rotor, ω_1 is the speed of stator, ω_s represents rotor's angular velocity.

The flux linkage equation is

$$\psi_{sd} = L_s i_{sd} + L_m i_{rd} \tag{5}$$

$$\psi_{sq} = L_s i_{sq} + L_m i_{rq} \tag{6}$$

$$\psi_{rd} = L_m i_{sd} + L_r i_{rd} \tag{7}$$

$$\psi_{rq} = L_m i_{sq} + L_r i_{rq} \tag{8}$$

where ψ_{sd}, ψ_{sq} are stator flux linkage of $d-$ and $q-$axis, ψ_{rd}, ψ_{rq} are rotor flux linkage of $d-$ and $q-$axis, L_s, L_r are inductance of stator and rotor, L_m represents mutual inductance.

The torque equation of the DFIG-based WT is as follows

$$T_m = T_e + \frac{J}{n_p}\frac{d\omega_r}{dt} \tag{9}$$

$$T_e = n_p L_m \left(i_{sq} i_{rd} - i_{sd} i_{rq}\right) \tag{10}$$

where T_m is WT's mechanical torque, T_e is generator's electromagnetic torque, J is rotor moment of inertia, ω_r is rotor moment of inertia, n_p is pole logarithm.

The DFIG-based WT's active and reactive power output are

$$P_s = u_{sd} i_{sd} + u_{sq} i_{sq} \tag{11}$$

$$Q_s = u_{sq} i_{sd} - u_{sd} i_{sq} \tag{12}$$

The mutual inductance decoupling of the stator and rotor windings is realized by Park transformation.

3. System model

3.1. HMIDC system model

The HMIDC system established in this paper is consist of VSC-HVDC system and LCC-HVDC system, which are fed into the same AC system with close electrical distance, as shown in Figure 2, $P_c + jQ_c$ is line load, X_T is line inductance, T_1, T_2 is transformer, respectively.

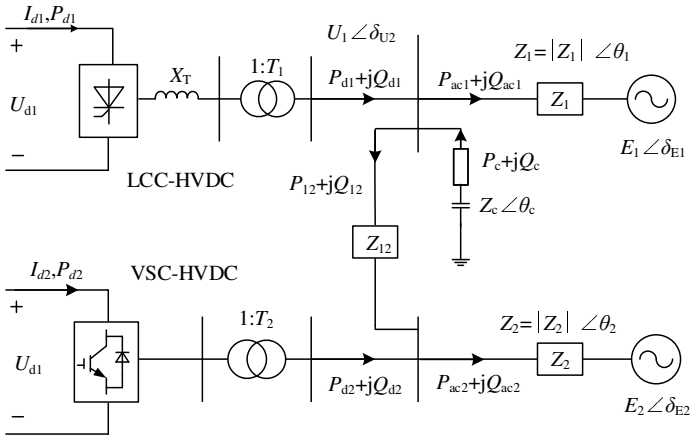

Figure 2. The HMIDC System

The LCC-HVDC rectifier side uses the control of constant DC current and minimum firing angle. The inverter side of LCC-HVDC uses constant DC current and fixed off angle control, current deviation control (CDC) [19]. Low voltage current limiting control (VDCOL) is adopted at both side to prevent the system's abnormal operation from being affected by low voltage. The parameters of VSC-HVDC system are selected based on the parameters of the International Council on Large Electric Systems (CIGRE) model. The parameters are shown as follows

Table 1: VSC control mode

Control Mode	Constant
1	Set active and AC voltage
2	Set constant DC voltage and AC voltage

3.2. The HMIDC system model with DFIG-based WT

For the purpose to analyze the influence of DFIG-based WT on the power grid, this paper uses the interconnected system consists of the HMIDC system, and the DFIG-based WT can be seen as follow. In Figure 3, ①, ②, and ③ indicate that the WTs are respectively connected in parallel at the VSC-HVDC sending end, the LCC-HVDC sending end, and the grid receiving end.

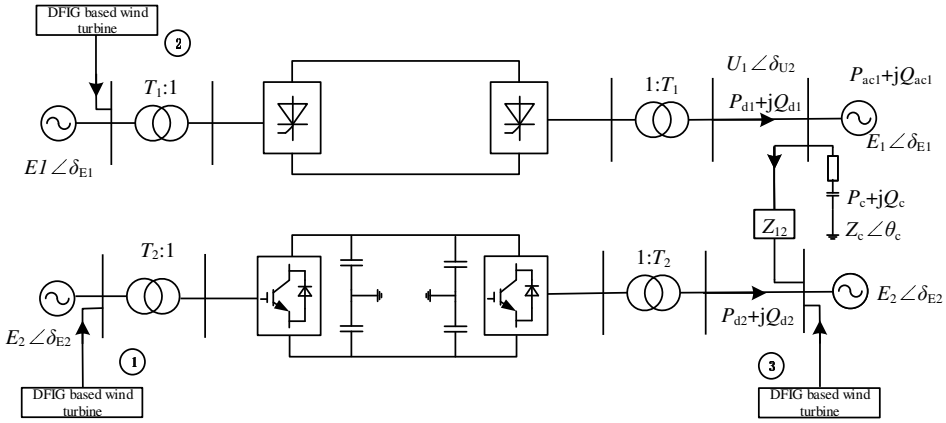

Figure 3. The HMIDC and DFIG-based WT connected to the Grid

4. Low frequency oscillation research method

The phenomenon of relative oscillation among generator rotors due to small disturbances is called LFO. The main cause of LFO is the negative damping effect of the power grid. Fast excitation systems and high-magnification excitation systems are more prone to negative damping. The decreasing of system damping is related to the weak connection of the power grid, the long-distance, and the overload power grid.

The universal analytical ways for LFO are eigenvalue analysis method, Prony analysis method. The eigenvalue analysis method can study the balance of the nonlinear system by analyzing the linearized system's stability. It mainly linearizes the system in the selected area, obtains the state equation of the system and calculates the eigenvalues of the matrix by calculation to analyze the oscillation mode, damping, frequency and sensitivity of the system. The Prony analysis method mainly selects an appropriate model order and data length for a given signal and calculates the amplitude, frequency, phase, and damping of the signal.

4.1 Characteristic value analysis method

In theory, small signal stability refers to the asymptotic stability of the traditional dynamic system in the Lyapunov sense [3]. On the basis of the Lyapunov method, the basic principles of power system stability are as follows:

The dynamic behavior of the system is represented by a series of nonlinear differential equations.

$$\frac{dx}{dt} = f\left(x_1, x_2, x_{3,\cdots}, x_n\right) i = 1,2,3,\cdots,n \tag{13}$$

Linearizing the equation and each state variable is represented by the sum of the initial amount and the increment as

$$x_i = x_{i0} + \Delta x_i \tag{14}$$

Ignoring the Taylor transform of the second and highest increments, the equation is

$$\frac{dx_i}{dt} = \sum_{j=1}^{n} \frac{\partial f_i}{\partial x_j} \Delta x_j i = 1,2,3,\cdots,n \tag{15}$$

The matrix can be rewritten as

$$\Delta X = B\Delta X \tag{16}$$

The above equation is the state equation representing the linear system, and B is the characteristic matrix of the network. The eigenvalues of the feature matrix can be derived from the state equation of the above equation. We can also use the matrix eigenvalues to judge the state of the system.

1) If at least one real part of the matrix eigenvalue is 0 and the rest are not greater than 0, it means that the system is running near the stable point, and the system is in a critical stable state.

2) If all the real parts of the system eigenvalue are less than 0, it represents that the system is running near the stable point, and the system is in a gradual stable state.

3) If more than one real parts of the eigenvalue is greater than 0, that is, the system is running near the stable point, and the system is unstable at this time.

Therefore, it can be determined whether the system is in a stable state by judging the eigenvalue of the system.

4.2. Damping ratio

By analyzing the damping ratio, the strength of the system damping can be judged. If the eigenvalue of the system is

$$\lambda_i = \alpha_i \pm j\omega_i \left(i = 1,2,\cdots,n\right) \tag{17}$$

The damping ratio ξ_i for the oscillation frequency ω_i is

$$\xi_i = \frac{-\alpha_i}{\sqrt{{\alpha_i}^2 + {\omega_i}^2}} \tag{18}$$

If $\xi_i \geq 0.1$, it represents that the system's characteristic of damping is strong; if $\xi_i < 0.03$, the damping in the system is weak. If $\xi_i \leq 0$, the damping in the system is negative, and the amplitude oscillation will occur.

5. Impact of wind farm on damping characteristics of the HMIDC system

In the HMIDC system, as the characteristics of the DFIG-based WT fluctuation, most of the wind farms have a long distance to the power generation center. Therefore, access point location and capacity of the WT have led to a growing concerning both impacts on the damping characteristics of the power network.

TLS-ESPRIT technology [20] is an effective method for identifying the oscillation characteristics of large systems with small disturbances. Compared with the traditional Prony algorithm, it has stronger identification ability and stronger anti-noise advantage. The main principle of the ESPRIT algorithm is to calculate the rotation factor by sampling the data to form the autocorrelation matrix and the cross-correlation matrix, and the signal from the rotation factor includes the frequency and attenuation factor. The amplitude and phase of the factor is able to be found by using TLS.

5.1. Impact of WT's location on system oscillation mode

It is a 1 MW, 0.69 kV DFIG-based WT unit. The model parameters are detailed in Table 2.

Table 2: Motor parameters

Parameter	Value
Blade radius *R*/m	40
Air density ρ/(kg▪m^3)	1.225
Rated wind speed/(m▪s^{-1})	12
Cut into wind speed/(m▪s^{-1})	11.5
Cut out wind speed/(m▪s^{-1})	10.5
Wind turbine rated speed ω_{mb}/(rad▪s^{-1})	1.1
Generator rated active power/MW	1
Generator rated voltage /kV	0.69
Stator winding resistance(pu)	0.0054
Rotor winding resistance (pu)	0.00607

This paper setting the wind speed to 11.5 m/s, and it becomes 10.5 m/s after 1s. A set of time-domain simulation data is first obtained when the DFIG-based WT unit is located at ① in Figure 3. Then a small disturbance excitation signal is applied to the WT. The specific implementation method is to set a single-phase ground fault at the wind turbine's access point to simulate the small interference signal of system, which is the circuit breaker is closed at 3s and opened after 0.2s, and another set of time-domain simulation data is obtained. The two sets of data of the generator power angle in the parallel position of the WT side are obtained. The TLS-ESPRIT method is used to identify the low frequency characteristic of the obtained data which is displayed as follow

Table 3: Oscillation model identification results

Oscillation Mode	Eigenvalue	Frequency/Hz	Damping ratio/%
Ultra-LFO mode	-0.6197±0.3957*i*	0.0630	84.2829
LFO mode 1	-1.6058±4.3202*i*	0.6876	34.8413
LFO mode 2	-1.5072±8.2714*i*	1.3164	17.9272
LFO mode 3	-1.3746±23.3952*i*	1.9728	11.0223
SSO mode 1	-1.0117±16.7822*i*	2.6710	6.0177
SSO mode 2	-0.6248±21.0927*i*	3.3570	2.9610

As we can see from Table 3 that there are six oscillation modes, the ultra-LFO mode with a frequency of 0.0630 Hz, the LFO mode of 0.6876 Hz, 1.3164 Hz and 1.9728 Hz, respectively. In other ways, the damping ratio becomes weaker as the frequency increases. In addition, there are sub-synchronous oscillations with frequencies of 2.6710 Hz and 3.3570 Hz. The damping ratios decrease with increasing frequency.

Similarly, the same method is used to obtain two sets of data of the generator power angle of the WT side parallel position when it is located at ② in Figure 3, and the TLS-ESPRIT method is used to identify the obtained data which is displayed as follow

. Table 4: Oscillation model identification results

Oscillation Mode	Eigenvalue	Frequency/Hz	Damping ratio/%
LFO mode 1	-1.3672±0.7056i	0.1123	88.8634
LFO mode 2	-0.4469±4.8817*i*	0.7769	9.1159
LFO mode 3	-0.9363±6.6574*i*	1.0596	13.9271
LFO mode 4	-1.0630±10.3559*i*	1.6482	10.2108
SSO mode 1	-0.8673±14.5406*i*	2.3142	5.9538
SSO mode 2	-0.5432±19.0112*i*	3.0257	2.8561

The Table 4 shows that there are six oscillation modes in the system, the LFO mode of 0.1123 Hz, 0.7769 Hz, 1.0596 Hz, 1.6482 Hz, the sub-synchronous frequency of 2.3142 Hz and 3.0257 Hz, respectively. The damping ratio gradually becomes weaker as the frequency increases.

When the WT is located at the power receiving end ③ of Figure 3, the oscillation mode identification result can be seen in Table 5.

Table 5: Oscillation model identification results

Oscillation Mode	Eigenvalue	Frequency/Hz	Damping ratio/%
Ultra-LFO mode	-0.0199±0.3583*i*	0.0570	5.5494
LFO mode 1	-0.5833±3.3023*i*	0.5256	17.3944
LFO mode 2	-0.0040±4.4469*i*	0.7077	0.0897
LFO mode 3	-0.7723±6.8079*i*	1.0835	11.27
LFO mode 4	-0.7641±10.5234*i*	1.6749	7.2419
SSO mode	-0.4956±14.8620*i*	2.3654	3.3331

The Table 5 shows that there are six oscillation modes in which there is one ultra-LFO mode with the frequency of 0.0570 Hz, and the rest are sub-synchronous oscillation modes with frequencies of 0.5256 Hz, 0.7077 Hz, 1.0835 Hz, 1.6749 Hz and 2.3654 Hz, respectively. As the frequency increases, the damping coefficient of the system gradually becomes weaker.

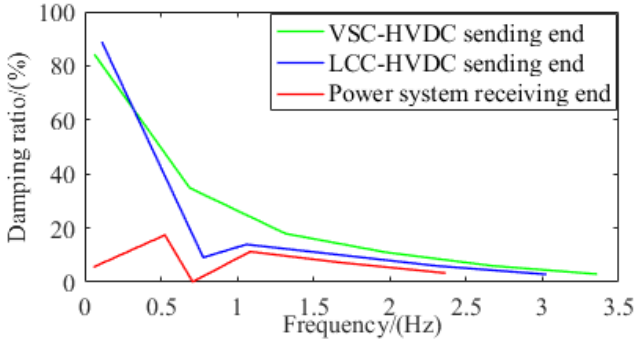

Figure 4. Different access point of DFIG-based WT

As can be seen from the above analyze that there are three kinds of oscillation modes: ultra-low frequency oscillation mode, LFO mode and sub-synchronous oscillation mode, and the damping ratio gradually declines with the increase of frequency when the WT is joined the HMIDC system from the VSC-HVDC sending end. The system has two oscillation modes: LFO mode and sub-synchronous oscillation mode, and the damping ratio gradually become weaker with the increase of the frequency when the WT is integrated into the HMIDC system from the LCC-HVDC sending end. The system has three kinds of oscillation modes: ultra-low frequency oscillation mode, LFO mode and sub-synchronous oscillation mode, and the damping ratio gradually becomes weaker as the frequency increases when the WT is integrated into the HMIDC system from the grid receiving end. The change of damping ratio is displayed in Figure 4.

5.2. Influence of WT capacity on the system mode

The effect of the HMIDC oscillation mode is analyzed by changing the capacity of the generator set. The simulation is carried out when the capacity of the WT is at different positions, and the capacity was increased from 1 MW to 10 MW. The TLS-ESPRIT method is used to recognize the LFO characteristics of the obtained data. The identification results are shown in Tables 6-8.

Table 6: Oscillation model identification results

Oscillation Mode	Eigenvalue	Frequency/Hz	Damping ratio/%
LFO mode 1	-0.6392±1.1671i	0.1857	48.04
LFO mode 2	-0.5102±6.0154i	0.9574	8.45
LFO mode 3	-0.0246±8.1508i	1.2972	0.3
LFO mode 4	-0.1128±9.4147i	1.4984	1.2

Table 6 shows how the change in the capacity of the WT causes a change in the system oscillation mode when the WT is located at ① of Figure 3. As we can see from Table 6 that

both ultra-low frequency oscillation mode and sub-synchronous oscillation mode in the original system disappear only the LFO mode exists. The damping gradually declines with the increase of the frequency which is almost zero.

Table 7: Oscillation model identification results

Oscillation Mode	Eigenvalue	Frequency/Hz	Damping ratio/%
LFO mode 1	-0.7534±1.8930i	0.3013	36.9783
LFO mode 2	-0.0369±3.8207i	0.6081	0.9665
LFO mode 3	-0.8534±5.7746i	0.9191	6.4629
LFO mode 4	-0.6401±9.8837i	1.5730	2.4822

Table 7 shows the change in the system oscillation mode caused by the alter in the capacity of the WT when it is located at ② of Figure 3. Similarly, an increase in the capacity of the WT results in the system having only a LFO mode, and the damping ratio become weak as the frequency increases.

Table 8: Oscillation model identification results

Oscillation Mode	Eigenvalue	Frequency/Hz	Damping ratio/%
LFO mode 1	-0.5921±3.3101i	0.5268	17.6096
LFO mode 2	-0.0506±0.3330i	0.7070	1.1385
LFO mode 3	-0.7614±6.8218i	1.0857	11.0919
LFO mode 4	-0.8044±10.5031i	1.6716	7.6359

Table 8 shows the alternation of the system oscillation mode result from the alter of the capacity of the WT when it is located at ③. As we can observe from Table 8 that when it is located at the receiving end grid, the increase of the wind turbine's capacity making only the LFO mode exist in the network, and the damping ratio is less than that in the WT with a capacity of 1 MW. The damping ratio decreases as the frequency increases.

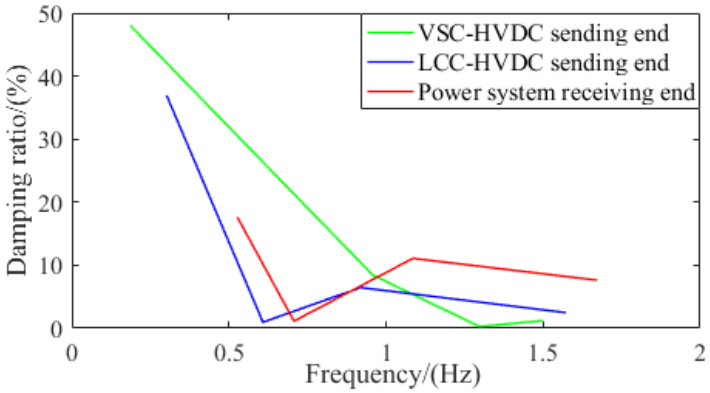

Figure 5. Different capacity of DFIG-based WT

As can be seen from the above analyze that after the wind turbine's capacity is increased from 1 WM to 10 MW, the system transitions from the original three oscillation modes to the LFO mode, and the damping ratio increases with frequency when it access to the VSC-HVDC sending end. And the system transitions from the original two oscillation modes to the LFO mode, and the damping ratio decreases as the frequency increases when it is

located at the LCC-HVDC sending end; the system consists of the original three oscillation modes transition to a LFO mode, and the damping ratio become weak as the frequency increases when it is located at the power receiving end. The change of damping ratio is displayed in Figure 5.

6. Conclusion

In this thesis, the model of HMIDC system with DFIG-based WT is established. Through the simulation in PSCAD/EMTDC platform, the corresponding power angle curve is obtained. The eigenvalues are identified by TLS-ESPRIT algorithm. The influence of wind turbine's access point and WT output on the oscillation characteristics of the power system is studied by eigenvalue analysis. The specific conclusions are:

1) Different access points of the DFIG-based WT will cause the system to produce different oscillation modes. The WTs are connected to the VSC-HVDC ① and the power system ③, respectively. The system has three oscillation modes. The WT is connected to the LCC-HVDC ②, and the system has only two oscillation modes. And in these oscillation modes, the damping ratio gradually decreases with increasing frequency.

2) At different access points, the modes of the power system are all LFO modes. The damping ratio decreases with increasing frequency when the capacity of the WT is increased from 1 WM to 10 MW. The change of damping ratio is not apparent than before.

Acknowledgment

This work was jointly supported by the National Nature Science Foundation of China (51607158), Key scientific and technological projects in Henan Province (192102210075, 192102310206), and key scientific and technological project of Henan Province (161100211600).

References

[1] Y. Long, J. Liu, W. Yao, J.Y. Wen. Complex Torque Analysis of the Influence Mechanism of Doubly-Fed Wind Turbine Running Speed on Its Shaft Oscillation [J]. *High Voltage Engineering*,2017,43(06):2088 - 2096.

[2] Q.Y. Jia. Study on Probability Small Interference Stability of AC/DC Hybrid System with Wind Farm [D]. *Shanghai University of Electric Power*, 2018.

[3] J.Y. Zou. Analysis of small disturbance stability and damping characteristics of doubly-fed wind turbine systems [D]. *Yanshan University*, 2015.

[4] L. Yang, X.N. Xiao, C.Z. Pang and C. Li, Effects of wind turbine generator's drive train model on sub-synchronous oscillation[C].2015 IEEE 2nd International Future Energy Electronics Conference (IFEEC), Taipei, 2015, pp. 1-6.

[5] G. Durga, V. Vijay, H. Terry. Impact of increased penetration of DFIG-based wind turbine generators on transient and small signal stability of power systems [J]. *IEEE Transactions on Power Systems*, 2009, 24(3) 14261434.

[6] A. K. Gupta, K. Verma and K. R. Niazi, "Impact analysis of DFIG location on low-frequency oscillations in power system," *The Journal of Engineering*, 2017, 2017(13): 1413-1417.

[7] A.C. Xue, Q. Wang, T.Q. Bi. Analysis of interaction mechanism of small disturbance power angle between double-fed wind turbine and synchronous machine [J]. *Proceedings of the CSEE*, 2016, 36(02): 417-425.

[8] H. Yu, G. Zhao, Y. Hu, B. Gao, X. Zhang and R. Zhang, "Damping characteristics of sub-synchronous torsional interaction of DFIG-based wind farm connected to HVDC system," *The Journal of Engineering*, 2016, 2017(13): 1934-1939.

[9] H. Li, H.W. Chen, C. Yang, B. Zhao, X.H. Tang. Analysis of Low Frequency Oscillation Mode of Power System with Doubly-Fed Wind Farm [J]. *Proceedings of the CSEE*, 2013, 33(28): 17-24+5.

[10] K. Sun, W. Yao, J. Fang, X. Ai, J. Wen and S. Cheng, "Impedance Modeling and Stability Analysis of Grid-Connected DFIG-Based Wind Farm With a VSC-HVDC," *IEEE Journal of Emerging and Selected Topics in Power Electronics*, 2020, 8(2): 1375-1390.

[11] B.H. Li, Y.M. Zhang, X.Y. Li, T.Q. Liu, R. Zhao. Design of reduced-order high-voltage DC additional controller based on improved projective control [J]. *Journal of Physics*, 2014, 63(09): 434-440.

[12] A. K. Gupta, K. Verma and K. R. Niazi. "Wide area coordinated control for low-frequency oscillations damping in a wind-integrated power system," *The Journal of Engineering*, 2019, 2019(18): 4941-4945.

[13] B.P. Chen, T. Lin, Y.S. Chen, J.N. Zhang, Y.B. Sheng, W.L. Xu. Parameter coordination of multi-channel additional damping controllers on the machine side and the grid side to suppress low-frequency oscillation and sub-synchronous oscillation [J]. *Electric Power Automation Equipment*, 2018, 38 (11): 50-56+62.

[14] B.P. Chen, T. Lin, R.S. Chen, J.N. Zhang and X.L. Xu. Coordinative optimization of multi-channel PSS and TCSC Damping Controller to suppress the low-frequency and sub-synchronous oscillation[C]. 2016 IEEE Power and Energy Society General Meeting (PESGM), Boston, MA, 2016, pp. 1-5.

[15] Y.J. Isbeih, M.S. El Moursi, W. Xiao and E. El-Saadany. "H∞ mixed-sensitivity robust control design for damping low-frequency oscillations with DFIG wind power generation," *IET Generation, Transmission& Distribution*, 2019, 13(19): 4274-4286.

[16] G. Zeng, X.Y. Li, T.Q. Liu, R. Zhao. Multi-channel wide-area adaptive damping control for suppressing low-frequency oscillation and sub-synchronous oscillation simultaneously [J]. *Journal of Physics*, 2014, 63(22): 428-436.

[17] B.P. Chen, T. Lin, Y.S. Chen, Z.Z Guo, Y.B. Sheng, Y.L. Xu. Analysis of Multi-band Oscillation Characteristics of Direct Drive Wind Farm via VSC-HVDC Grid-connected System [J]. *Transactions of China Electrotechnical Society*, 2018,33(S1): 176-184.

[18] L.H. Yang, X.K. Ma. Influence of doubly-fed wind turbines on low-frequency oscillation characteristics of power system[J]. *Proceedings of the CSEE*, 2011, 31(10): 19-25.

[19] C. Guo, W. Liu, J. Zhao and C. Zhao. Impact of control system on small-signal stability of hybrid multi-infeed HVDC system[J]. *IET Generation, Transmission & Distribution*, vol. 12, no. 19, pp. 4233-4239, 30 10 2018.

[20] B. Xu and Z. Zheng. SVD filtering and TLS-ESPRIT algorithm based on stator fault characteristic detection of doubly-fed induction generator [J]. *The Journal of Engineering*, vol. 2019, no. 18, pp. 5193-5196, 7 2019.